NOTE

An Integral Evolution Formula for the Wave Equation

Bradley Alpert,[*,1] Leslie Greengard,[†,2] and Thomas Hagstrom[‡,3]

[*]*National Institute of Standards and Technology, 325 Broadway, Boulder, Colorado 80303,* [†]*Courant Institute of Mathematical Sciences, New York University, 251 Mercer Street, New York, New York 10012-1110, and* [‡]*Department of Mathematics and Statistics, University of New Mexico, Albuquerque, New Mexico 87131*
E-mail: alpert@boulder.nist.gov, greengar@cims.nyu.edu, hagstrom@math.unm.edu

We present a new time-symmetric evolution formula for the scalar wave equation. It is simply related to the classical D'Alembert or spherical means representations, but applies equally well in two space dimensions. It can be used to develop stable, robust numerical schemes on irregular meshes. ⓒ 2000 Academic Press

Key Words: small-cell problem; stability.

1. INTRODUCTION

It is notoriously difficult to construct stable high-order explicit marching schemes for the wave equation on irregular meshes. The time-step restriction is typically determined by the smallest cell present in the discretization. In this note, we describe a new approach to the construction of stable, explicit schemes, based on a simple time-symmetric evolution formula.

Initially we consider the Cauchy problem in $\mathbf{R}^d$,

$$
\begin{aligned}
u_{tt} &= \Delta u, \\
u(\mathbf{x}, 0) &= u_0(\mathbf{x}), \\
u_t(\mathbf{x}, 0) &= v_0(\mathbf{x}),
\end{aligned}
\tag{1}
$$

where Δ denotes the Laplacian operator. In one space dimension, the solution can be written using D'Alembert's formula as

$$
u(x, t) = \frac{1}{2}(u_0(x - t) + u_0(x + t)) + \int_{x-t}^{x+t} v_0(s)\, ds.
\tag{2}
$$

We can eliminate the term involving the data $v_0(x)$ by using the time-symmetric form:

$$
u(x, t) + u(x, -t) = u(x - t, 0) + u(x + t, 0).
\tag{3}
$$

In three dimensions, the analog of (3) is the spherical means formula [2, 4, 5]

$$
u(\mathbf{x}, t) + u(\mathbf{x}, -t) = \frac{\partial}{\partial t}\left[\frac{t}{4\pi} \int_{|\mathbf{y}-\mathbf{x}|=t} u(\mathbf{y}, 0)\, d\sigma\right],
\tag{4}
$$

where $d\sigma$ is an element of surface area. In two dimensions, the situation is slightly more complex because of the absence of a strong Huygen's principle. The solution depends not just on function values over the boundary of the disk of radius t, but on all values in its interior:

$$
u(\mathbf{x}, t) + u(\mathbf{x}, -t) = \frac{\partial}{\partial t}\left[\frac{1}{2\pi} \int_{|\mathbf{y}-\mathbf{x}|\leq t} \frac{u(\mathbf{y}, 0)}{\sqrt{t^2 - |\mathbf{x} - \mathbf{y}|^2}}\, d\mathbf{y}\right].
\tag{5}
$$

For numerical computation, formulas of the types (3), (4), and (5) are not widely used because they do not suggest a procedure at physical boundaries and are not easily extended to more general partial differential equations.

2. A CENTRAL DIFFERENCE EVOLUTION FORMULA

Consider the Fourier transform of the wave function $u(\mathbf{x}, t)$, namely

$$
U(\mathbf{k}, t) = \left(\frac{1}{\sqrt{2\pi}}\right)^d \int_{\mathbf{R}^d} e^{-i\mathbf{k}\cdot\mathbf{x}} u(\mathbf{x}, t)\, d\mathbf{x}.
$$

The partial differential equation in (1) can then be replaced by

$$
U_{tt}(\mathbf{k}, t) = -|\mathbf{k}|^2 U(\mathbf{k}, t).
$$

Solving this ordinary differential equation, we obtain

$$
U(\mathbf{k}, t) + U(\mathbf{k}, -t) = 2U(\mathbf{k}, 0)\cos(|\mathbf{k}|t)
$$

or

$$U(\mathbf{k}, t) - 2U(\mathbf{k}, 0) + U(\mathbf{k}, -t) = \left[\frac{2\cos(|\mathbf{k}|t) - 2}{-|\mathbf{k}|^2} \right] (-|\mathbf{k}|^2) U(\mathbf{k}, 0). \tag{6}$$

Our main result follows.

THEOREM 2.1. *Let $u(\mathbf{x}, t)$ denote a solution to the homogeneous wave equation*

$$u_{tt} = \Delta u$$

in $\mathbf{R}^d$. Then

$$u(\mathbf{x}, t) - 2u(\mathbf{x}, 0) + u(\mathbf{x}, -t) = \int_{|\mathbf{y}-\mathbf{x}| \le t} G_d(|\mathbf{x} - \mathbf{y}|, t) \Delta u(\mathbf{y}, 0) \, d\mathbf{y}, \tag{7}$$

where

$$G_1(r, t) = t - r \tag{8}$$

$$G_2(r, t) = \frac{1}{\pi} \ln(t + \sqrt{t^2 - r^2}) - \frac{1}{\pi} \ln r \tag{9}$$

$$G_3(r, t) = \frac{1}{2\pi} \tag{10}$$

Proof. Formula (7) is obtained from the convolution theorem by transforming (6) back to physical space. We provide a few more details for two space dimensions, where we need to evaluate the kernel

$$G_2(|\mathbf{x}|, t) = \frac{1}{(2\pi)^2} \int_{-\infty}^{\infty} \int_{-\infty}^{\infty} \left[\frac{2\cos(|\mathbf{k}|t) - 2}{-|\mathbf{k}|^2} \right] \cdot e^{i\mathbf{k}\cdot\mathbf{x}} \, d\mathbf{k}.$$

Changing to polar coordinates, we have

$$G_2(r, t) = \frac{1}{(2\pi)^2} \int_0^{\infty} \int_0^{2\pi} \left[\frac{2 - 2\cos(kt)}{k^2} \right] e^{ikr\cos(\theta-\phi)} k \, dk \, d\phi$$

$$= \frac{1}{2\pi} \int_0^{\infty} \left[\frac{2 - 2\cos(kt)}{k} \right] J_0(kr) \, dk,$$

where $\mathbf{k} = (k\cos\phi, k\sin\phi)$, $\mathbf{x} = (r\cos\theta, r\sin\theta)$, and J_0 denotes the Bessel function of order zero. The desired result now follows from the formula [1, 6.693]

$$\int_0^{\infty} J_\nu(kr) \cos(kt) \frac{dk}{k} = \begin{cases} \dfrac{1}{\nu} \cos\left(\nu \arcsin \dfrac{t}{r} \right) & t \le r \\[3mm] \dfrac{r^\nu}{\nu(t + \sqrt{t^2 - r^2})^\nu} \cos \dfrac{\nu\pi}{2} & t \ge r, \end{cases}$$

with some care in taking the limit $\nu \to 0$. ∎

Remark. Integration by parts and Green's identities can be used to recover the formulas (3), (4), and (5) from (7).

Remark. Our evolution scheme can be viewed as an integral form of the widely-used Lax–Wendroff method. This method uses central differencing in time to generate the series

$$u(\mathbf{x}, t) - 2u(\mathbf{x}, 0) + u(\mathbf{x}, -t) = t^2 u_{tt}(\mathbf{x}, 0) + \frac{t^4}{12} u_{tttt}(\mathbf{x}, 0) + \frac{t^6}{360} u_{tttttt}(\mathbf{x}, 0) + \cdots.$$

Replacing the time derivatives with powers of the Laplacian, one obtains

$$u(\mathbf{x}, t) - 2u(\mathbf{x}, 0) + u(\mathbf{x}, -t) = t^2 \Delta u(\mathbf{x}, 0) + \frac{t^4}{12} \Delta^2 u(\mathbf{x}, 0) + \frac{t^6}{360} \Delta^3 u(\mathbf{x}, 0) + \cdots.$$

Once a numerical approximation is chosen for the Laplacian operator, the Lax–Wendroff scheme achieves arbitrary order accuracy in time by incorporating higher and higher powers of the Laplacian in a three time level scheme. Stability and spatial accuracy depend, of course, on how the Laplacian is computed.

3. FORCING

We next consider the wave equation with a source term

$$u_{tt} = \Delta u + f \tag{11}$$

which from Fourier transformation $(u \to U, \; f \to F)$ becomes

$$U_{tt}(\mathbf{k}, t) = -|\mathbf{k}|^2 U(\mathbf{k}, t) + F(\mathbf{k}, t),$$

whose solution is given by

$$U(\mathbf{k}, t) - 2U(\mathbf{k}, 0) + U(\mathbf{k}, -t)$$
$$= 2[\cos(|\mathbf{k}|t) - 1]U(\mathbf{k}, 0) + \int_{-t}^{t} \frac{\sin(|\mathbf{k}|(t - |s|))}{|\mathbf{k}|} F(\mathbf{k}, s) \, ds.$$

The identity

$$\frac{\sin(|\mathbf{k}|t)}{|\mathbf{k}|} = -\frac{\partial}{\partial t} \left(\frac{\cos(|\mathbf{k}|t) - 1}{|\mathbf{k}|^2} \right)$$

and integration by parts, in combination with (7), now yield

THEOREM 3.1. *Let $u(\mathbf{x}, t)$ denote a solution to the inhomogeneous wave equation* (11) *in $\mathbf{R}^d$. Then*

$$u(\mathbf{x}, t) - 2u(\mathbf{x}, 0) + u(\mathbf{x}, -t)$$
$$= \int_{|\mathbf{y}-\mathbf{x}| \leq t} G_d(|\mathbf{x} - \mathbf{y}|, t)[\Delta u(\mathbf{y}, 0) + f(\mathbf{y}, 0)] \, d\mathbf{y}$$
$$+ \frac{1}{2} \int_{-t}^{t} \text{signum}(s) \int_{|\mathbf{y}-\mathbf{x}| \leq t - |s|} G_d(|\mathbf{x} - \mathbf{y}|, t - |s|) f'(\mathbf{y}, s) \, d\mathbf{y} \, ds, \tag{12}$$

where G_d is given in (8)–(10) *and $f'(\mathbf{x}, t) = \partial f(\mathbf{x}, t)/\partial t$.*

Remark. The derivative f' of the forcing term may be analytically removed from (12) by integration, yielding formulas that differ somewhat for $d = 1, 2, 3$. In three dimensions, for example, the double integral reduces to the particularly simple form

$$\frac{1}{2} \int_{|\mathbf{y} - \mathbf{x}| \leq t} \frac{f(\mathbf{y}, |\mathbf{x} - \mathbf{y}| - t) - 2f(\mathbf{y}, 0) + f(\mathbf{y}, t - |\mathbf{x} - \mathbf{y}|)}{|\mathbf{x} - \mathbf{y}|} \, d\mathbf{y}.$$

4. DISCRETIZATION

In order to use formula (7) or (12) for computation, we need to evaluate the integral

$$Q_u(\mathbf{x}) = \int_{|\mathbf{y} - \mathbf{x}| \leq t} G_d(|\mathbf{x} - \mathbf{y}|, t) \Delta u(\mathbf{y}, 0) \, d\mathbf{y}, \tag{13}$$

for each discretization point $\mathbf{x}$. In this brief note, we will restrict our attention to the one-dimensional case. Away from physical boundaries, there are three clear options:

1. Use a quadrature formula designed for formula (13):

$$Q_u(x) = \int_{x-t}^{x+t} (t - |y - x|) u_{yy}(y, 0) \, dy. \tag{14}$$

2. Integrate by parts once to obtain

$$Q_u(x) = -\int_{x-t}^{x} u_y(y, 0) \, dy + \int_{x}^{x+t} u_y(y, 0) \, dy. \tag{15}$$

3. Integrate by parts twice to obtain

$$Q_u(x) = u(x - t, 0) - 2u(x, 0) + u(x + t, 0).$$

All three formulas are exact (the last yielding the time-symmetric scheme (3)). In the first case, one needs to approximate u_{xx} within the domain of dependence. In the second case, one needs to approximate u_x within the domain of dependence. In the third case, one needs to interpolate $u(x - t, 0)$ and $u(x + t, 0)$ from the possibly irregular mesh points where $u(x, 0)$ is known. The stability of each scheme will depend on how the interpolation–approximation problem is handled.

To demonstrate the value of the integral formulation, we suppose that we are solving the problem (1) with the Dirichlet boundary condition $u(0, t) = g(t)$. For the sake of simplicity, we assume that the grid spacing in x is equal to the time step t. The only irregular point is the first grid point x_1 which is arbitrarily close to the boundary $x = 0$, creating what is often referred to as a *small cell* problem (Fig. 1).

For nodes other than x_1, we can use any of the three options outlined above. For $x \leq x_1 \leq t$, let us define

$$\tilde{u}(x, \tau) = 2u(x, 0) - u(x, -\tau) + \int_{0}^{x+\tau} (\tau - |y - x|) u_{yy}(y, 0) \, dy. \tag{16}$$

Note that $\tilde{u}$ satisfies the wave equation exactly, under the assumption that the function $u_{xx}(x, 0)$ is extended outside the domain $x \geq 0$ by zero. Taking into account the Dirichlet
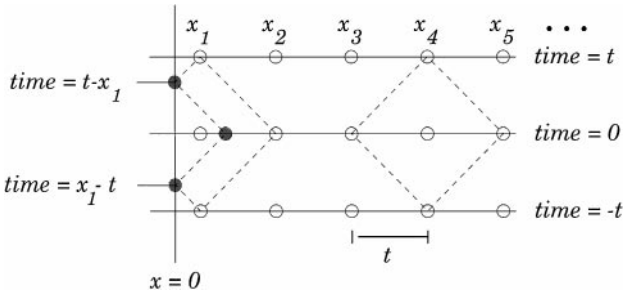
FIG. 1. An irregular mesh in one space dimension. The grid points $x_1, x_2, x_3, \ldots$ are equispaced, but the first grid point is near the physical boundary $x = 0$. At regular grid points, the symmetric stencil (3) is used. For the node x_1, the interpolatory scheme described in Section 4.2 uses the indicated stencil. It requires values at the irregular points marked by darkened circles.

data, it is straightforward to verify that the exact solution is

$$u(x_1, t) = \tilde{u}(x_1, t) + g(t - x_1) - \tilde{u}(0, t - x_1). \tag{17}$$

4.1. Quadrature Schemes

The most straightforward use of the quadrature approach is to compute u_{xx} at time $t = 0$ by a finite difference method of kth order accuracy. We can then integrate the formula (14) or (16) exactly for a polynomial approximant of u_{xx} of degree $k - 1$. For $k = 2$ this involves computing the second derivative using the usual three-point stencil at regular grid points and a one-sided four-point stencil for the irregular points $x = 0, x_1$. The necessary quadratures are easy to derive for a piecewise linear approximation of u_{xx}.

4.2. Interpolation Schemes

Integrating by parts yet again, we can rewrite the formula (16) for $\tilde{u}(x_1, t)$ as

$$\tilde{u}(x_1, t) = -u(x, -t) + u(x_1 + t, 0) + u(0, 0) - (t - x_1)u_x(0, 0).$$

Combining this result with (17), we have

$$u(x_1, t) = -u(x_1, -t) + u(x_1 + t, 0) + g(t - x_1) + g(-t + x_1) + u(t - x_1, 0). \tag{18}$$

For regular grid points, we use the exact formula (3). Once we choose a method for approximating the values $g(t - x_1)$, $g(-t + x_1)$, and $u(t - x_1, 0)$, we have a well-defined evolution scheme. In our numerical experiments, we assume the Dirichlet data $g(t)$ is known analytically, so that we only need to interpolate $u(t - x_1, 0)$.

4.3. Extrapolation Schemes

As a final alternative, one can try to use the time symmetric formula (3) for all grid points. This involves the value $u(x_1 - t, 0)$, which requires extrapolation from the known data at $x = 0, x_1, x_2, \ldots$.

TABLE I

Performance of the Quadrature, Interpolation, Extrapolation, and Leapfrog Schemes

N	$E_2(Q2)$	$E_2(I1)$	$E_2(I3)$	$E_2(X1)$	$E_2(LF2)$
16	$0.58 \cdot 10^{-4}$	$0.31 \cdot 10^{-6}$	$0.79 \cdot 10^{-10}$	$0.17 \cdot 10^{54}$	$0.35 \cdot 10^{75}$
32	$0.12 \cdot 10^{-4}$	$0.16 \cdot 10^{-6}$	$0.97 \cdot 10^{-11}$	$0.39 \cdot 10^{104}$	$0.42 \cdot 10^{150}$
64	$0.28 \cdot 10^{-5}$	$0.81 \cdot 10^{-7}$	$0.11 \cdot 10^{-11}$	—	—
128	$0.67 \cdot 10^{-6}$	$0.41 \cdot 10^{-7}$	$0.14 \cdot 10^{-12}$	—	—
256	$0.16 \cdot 10^{-6}$	$0.19 \cdot 10^{-7}$	$0.27 \cdot 10^{-13}$	—	—

Note. The first column lists the number of subintervals in the uniform grid region. The second through the fifth columns list the L_2 error from using the indicated evolution scheme after N steps.

5. A NUMERICAL EXAMPLE

We have implemented simple versions of the various methods described above: the second order quadrature scheme ($Q2$), the interpolation scheme using linear and cubic interpolation ($I1$, $I3$), and the extrapolation scheme using linear approximation ($X1$). For the sake of comparison, we use the same values of u_{xx} as in the quadrature approach, but march using the simplest leapfrog scheme [3]

$$\tilde{u}(x, t) = 2u(x, 0) - u(x, -t) + t^2 u_{xx}(x, 0). \tag{19}$$

We will denote this method by $LF2$.

We consider the wave equation on [0, 1] as an initial–boundary-value problem with exact solution $\sin(x - t) + \sin(x - t - \frac{1}{2})$. We set $x_1 = 1.0 \cdot 10^{-5}$, $x_{N+1} = 1 - 1.0 \cdot 10^{-6}$, and place $N - 1$ equispaced points on the interval $[x_1, x_{N+1}]$. With $N = 16, 32, 64, 128, 256$, both the first and the last cells are extremely small in comparison with $\Delta t = (x_{N+1} - x_1)/N$. The calculation is terminated after N steps, at which point we measure the L_2 error of the solution. The scheme used at the right boundary ($x = 1$) is analogous to the one described above at the left boundary ($x = 0$).

Results of the methods $Q2$, $I1$, $I3$, $X1$, $LF2$ are summarized in Table I.

$Q2$, $I1$, and $I3$ appear to be stable, while both the extrapolation and the leapfrog schemes diverge. It is also worth noting that $Q2$ is globally second order accurate, $I1$ is globally first order accurate, and $I3$ is globally third order accurate. This is consistent with a straightforward local error analysis. The reason that the first order scheme $I1$ is more accurate than $Q2$ for small N is that we are using an exact formula away from the irregular nodes in the former and a second order accurate quadrature at all points in the latter.

6. CONCLUSIONS

We have derived a new exact representation for solutions of the wave equation. Theorems 2.1 and 3.1 may be of analytical interest in their own right, but we have concentrated in this note on exploring some numerical consequences. We believe that marching schemes based on this approach have advantageous stability properties when compared to existing methods, most notably in removing the small cell problems which arise when using unstructured grids or regular Cartesian meshes in complex geometries. Although small cells can be easily eliminated in one dimension, at some cost in accuracy, doing so in two or three

dimensions is more complicated and results in greater loss of accuracy. Furthermore, higher-order discretizations *require* small cells near the boundary to avoid the Runge phenomenon.

We have illustrated the advantages in the simplest one-dimensional model problem, but the extension to higher dimensions is straightforward. Suppose, for example, that we are solving the wave equation in a domain $\Omega \subset \mathbf{R}^d$. If a point $\mathbf{x}$ is within a time step t of the domain boundary $\partial\Omega$, we define the function

$$\tilde{u}(\mathbf{x}, \tau) = 2u(\mathbf{x}, 0) - u(\mathbf{x}, -\tau) + \int_{S_\tau \cap \Omega} G_d(|\mathbf{x} - \mathbf{y}|, \tau)\Delta u(\mathbf{y}, 0)\, d\mathbf{y}, \qquad (20)$$

where $S_\tau = \{\mathbf{y} : |\mathbf{y} - \mathbf{x}| \le \tau\}$. Whereas in one dimension, the exact solution is given by (17), it is now of the form

$$u(\mathbf{x}, t) = \tilde{u}(\mathbf{x}, t) + B(\partial\Omega, \tilde{u}, g). \qquad (21)$$

The operator $B(\partial\Omega, \tilde{u}, g)$ describes the exact solution to the Dirichlet problem with zero initial data and boundary condition $g(\mathbf{x}, t) - \tilde{u}(\mathbf{x}, t)$. This can be written out explicitly in terms of hyperbolic potential theory and can easily be generalized to Neumann or Robin boundary value problems.

It is not surprising, perhaps, that robustness and stability come at a price. In our formulation, that price is the construction of appropriate quadratures for both the volume integral in (20) and the boundary operator $B(\partial\Omega, \tilde{u}, g)$ in (21). Higher dimensional examples, higher-order discretizations, and stability estimates will be reported at a later date.

REFERENCES

1. I. S. Gradshteyn and I. M. Ryzhik, *Tables of Integrals, Series, and Products* (Academic Press, New York, 1980).

2. P. R. Garabedian, *Partial Differential Equations* (Wiley, New York, 1964).

3. A. Iserles, *A First Course in the Numerical Analysis of Differential Equations* (Cambridge Univ. Press, Cambridge, UK, 1996).

4. F. John, *Partial Differential Equations* (Springer-Verlag, New York, 1982).

5. F. John, *Plane Waves and Spherical Means Applied to Partial Differential Equations* (Interscience, New York, 1955).